

Frictional behaviour of three critical geosynthetic interfaces

B. M. Bacas¹, J. Cañizal² and H. Konietzky³

¹Civil Engineer, Geotechnical Engineering Terrasolum S.L. Technology Development Center of University of Cantabria (CDTUC) Mod 107, Avda. los Castros s/n 39005 Santander, Spain, Telephone: +34942272685; Telefax: +34942272685; E-mail: bacasb@terrasolum.es (corresponding author)

²Professor of Geotechnical Group, School of Civil Engineering of University of Cantabria. Avda. los Castros s/n 39005 Santander, Spain, Telephone: +34942201813; Telefax: +34942201821; E-mail: canizalj@unican.es

³Professor and Chair for Rock Mechanics, Geotechnical Institute. TU Bergakademie Freiberg. Gustav-Zeuner-Str. 1, D-09596 Freiberg, Germany, Telephone: +493731393453; Telefax: +493731393501; E-mail: heinz.konietzky@ifgt.tu-freiberg.de

Received 13 January 2015, revised 30 April 2015, accepted 10 May 2015, published 11 August 2015

ABSTRACT: This paper's scope is the shear interaction mechanisms of three critical geosynthetic interfaces (geotextile/geomembrane; drainage geocomposite/geomembrane and soil/geomembrane) typically used for lined containment facilities such as landfills. A large direct shear machine was used to carry out 159 geosynthetic interface tests. The results showed strain softening behaviour, a very small dilatancy, 0.1–1 mm, and non-linear failure envelopes at normal stress range of 25–500 kPa. The three types of interfaces present the same main interaction mechanisms: interlocking and friction. For geotextile/geomembrane and drainage geocomposite/geomembrane interfaces, the higher the asperity height, the higher the interface shear strength. Whereas for soil/geomembrane interfaces, the higher the soil shear strength, the higher the interface shear strength. The drainage geocomposite/geomembrane interface showed the lowest friction angles, followed by the geotextile/geomembrane and the soil/geomembrane interfaces.

Keywords: Geosynthetics, Interface shear strength, Friction angle, Critical interfaces, Direct shear test

REFERENCE: Bacas, B. M., Cañizal, J. and Konietzky, H. (2015). Frictional behaviour of three critical geosynthetic interfaces. *Geosynthetics International*, 22, No. 5, 355–365. [<http://dx.doi.org/10.1680/gein.15.00017>]

1. INTRODUCTION

The main functions of a municipal solid waste landfill are: maximum accumulation of waste in the smallest possible space, isolation the waste from natural surroundings and maintaining security as well as future possible usage after its closure. Landfills are mainly isolated by geosynthetic protection layers, which interact on geosynthetic/geosynthetic and geosynthetic/soil interfaces. It is known that to ensure stability of a landfill, knowledge of the shear behaviour of these interfaces is critical. This issue has been investigated thoroughly in recent decades (some of the most recent papers are Fox and Kim (2008), McCartney *et al.* (2009), Palmeira (2009), Eid (2011), Fox and Ross (2011), Brachman and Sabir (2013), Vieira *et al.* (2013), Liu and Martinez (2014), Sayeed *et al.* (2014), Fox and Stark (2015)).

The objective of this paper was to study the shear behaviour of three critical geosynthetic interfaces, geotextile/geomembrane (GT/GM), drainage geocomposite/geomembrane (GC/GM) and soil/geomembrane (soil/GM),

providing an even deeper understanding than those presented in other studies. The large direct shear test has been used to carry out this testing programme since the applied normal stress range was between 25 and 500 kPa. Both Giroud *et al.* (1990) and Briançon *et al.* (2011) pointed out that for very low normal stress (lower than 25 kPa), the inclined plane test should be used.

The GT/GM interfaces can be used for both, lining and cover systems of the landfills. Geomembranes are typically used as a hydraulic barrier and geotextiles protect it from damage that may occur in some situations, such as high normal stresses and angular soil particles. These types of interfaces have been previously studied by Giroud *et al.* (1990), Koutsourais *et al.* (1991), Giroud and Darrasse (1993), Gilbert and Byrne (1996), Stark *et al.* (1996), Jones and Dixon (1998), Wasti and Özdüzgün (2001), Hebler *et al.* (2005), Bergado *et al.* (2006), Pitanga *et al.* (2009) and Kim and Frost (2011). The GT/GM interface was studied by means of the results of eighteen different interfaces using three types of geotextiles and five types of geomembranes.

The drainage GC/GM interfaces are widely used in landfill sealings, especially in cover systems. This interface minimises rainfall infiltration into a solid waste landfill. The geocomposite prevents the water from flowing into the waste. GC/GM interfaces have been investigated by Giroud *et al.* (1990) and Stark *et al.* (1996). This kind of interface was analysed with twelve different interfaces using two types of geocomposites and five types of geomembranes.

Lastly the soil/GM interfaces are an important part of the landfills' foundation and are also used to waterproof reservoirs. The soil is heavily compacted creating a geologic barrier to prevent the leachate from reaching the natural ground. Soil/GM interfaces have been studied by Seed and Boulanger (1991), Stark and Poeppel (1994), Zettler *et al.* (2000), Sharma *et al.* (2007), Eid (2011) and Fox *et al.* (2011). This type of interface was investigated by means of eleven different interfaces using three different soils and five types of geomembranes.

In the present study a methodology based on the ASTM D5321 was applied to carry out direct shear tests for different types of interfaces. The means to grip the different geosynthetics inside the shear box and the suitable test parameters (shear displacement rate, consolidation time and hydration time) were established based on studies from Stark and Poeppel (1994), Stark *et al.* (1996), Fox *et al.* (1997), Jones and Dixon (1998), Fox *et al.* (1998), Eid *et al.* (1999), Triplett and Fox (2001), Zornberg *et al.* (2005), Sharma *et al.* (2007) and McCartney *et al.* (2009). The relationships analysed were the interface shear strength versus shear displacement, the shear displacement versus normal displacement and the interface shear strength versus normal stress.

2. EXPERIMENTAL WORK

2.1. Materials

Table 1 presents the physical characteristics of different types of geosynthetics that were used for the direct shear tests.

- Three nonwoven geotextiles: GT1 (500 g/m²) was made of needle-punched monofilaments; GT2 (500 g/m²) was made of needle-punched staple fibres and GT3 (335 g/m²) was made of thermally bonded monofilaments.
- Five geomembranes, 1.5 mm thick: GM had smooth surfaces; GMr1 and GMr4 had irregular heavy textured surfaces smaller than 1 mm; GMr2s1 and GMr3 showed regular evenly spread asperities larger than 1 mm; GMr2s2 exhibited regular spread asperities smaller than 1 mm.
- Two drainage geocomposites: GC1 consisted of two nonwoven needle-punched geotextiles (200 and 300 g/m²) thermally bonded to a geonet. GC2 consisted of two nonwoven needle-punched geotextiles (120 and 140 g/m²) thermally bonded to a geonet. The type of geonet was the same for both geocomposites. The geonet had two strands with an angle of 70° in the

machine direction and 110° in the cross machine direction.

Table 2 presents the characteristics of the three soils employed for testing, which were part of the foundation of three landfills in Spain. The soil S1 and S2 came from landfills in Cataluña and S3 came from a landfill in Albacete. The soil S3 presented a larger plasticity index than S1 and S2.

Tables 3, 4 and 5 summarise the different GT/GM, GC/GM and soil/GM interfaces tested as well the testing conditions.

2.2. Testing equipment

The tests on geosynthetics were carried out with a large direct shear machine. The shear box was 300 mm long and 300 mm wide and therefore fulfilled the minimum requirement. The tests were performed with a constant shear rate and fixed normal stress. The shear box was divided into a moving lower part and a static upper part. One geosynthetic was fastened to the lower box, whereas the other one was fastened to the upper box. Different gripping systems were used for the different types of geosynthetics. The geotextiles were gripped with a double-sided adhesive tape. This system worked well for the range of normal stresses tested.

Based on the studies of Fox *et al.* (1997, 1998) a particularly textured plate was designed to grip the geosynthetic clay liners, drainage geocomposites and geomembranes. The dimension of this plate was 300 mm × 285 mm × 10 mm. The top face had pyramids of 1 mm height placed quincunx. The bottom face had channels that ran along the drainage holes allowing the water flow (Bacas *et al.* 2011). This piece was screwed on to a metal support that was placed into the direct shear box. The top side was in contact with the geosynthetic and the bottom side was in contact with the metal support. Figure 1 shows three sketches of the arrangement of the geosynthetic samples inside the direct shear machine.

2.3. Procedures

The direct shear tests were performed in accordance with the ASTM D5321 method.

The GT/GM interfaces were tested under wet conditions (Table 3) and the drainage GC/GM were tested under dry conditions (Table 4). It is worth mentioning the studies of Byrne *et al.* (1992), Mitchell and Mitchell (1992) and Bergado *et al.* (2006) in which they showed that the water content did not significantly affect the interface shear strength. The soil/GM interfaces were tested under dry conditions (Table 5) because both the compacted soil and geomembranes were highly impermeable and the interface would require a lot of time to be saturated.

The hydration time was 24 h for geotextiles, these samples were submerged into tap water inside a humid chamber (temperature 21°C, humidity 96%). The geomembranes were not hydrated. The consolidation time was 10 min inside the shear machine and the constant shear rate was 5 mm/min for GT/GM and GC/GM and

Table 1. Type of geosynthetics

Geosynthetic	Label	Type ^a	Raw material ^b /Type of fibre	Manufacturing process	Mass/area or density	Thickness ^c (mm)
Geotextiles	GT1	NW	PP/monofilament	Needle-punched	500 g/m ²	4 ± 0.2
	GT2	NW	PP/staple fibres	Needle-punched	500 g/m ²	5 ± 0.6
	GT3	NW	70%PP 30%PE /monofilament	Thermally bonded	335 g/m ²	2 ± 0.2
Geomembranes	GMr1	Textured (~0.5 mm) ^d	HDPE	Coextrusion with nitrogen gas	≥ 0.94 g/cm ³	1.5
	GMr2	Textured (s1:~1.2; s2:~0.8) ^d	HDPE	Calendered structured	≥ 0.94 g/cm ³	1.5
	GMr3	Textured (~1.3)	HDPE	Structured same resin as base	0.94 g/cm ³	1.5
	GMr4	Textured (~0.25)	HDPE	Coextrusion with nitrogen gas	≥ 0.93 g/cm ³	1.4
Drainage Geocomposite	GMs	Smooth	HDPE	Flat sheet extrusion	0.94 g/cm ³	1.5
	GC1	NW(200)/Geonet/ NW(300)	PP (geotextile), HDPE (geonet)	Thermally bonded	950 g/m ²	5
	GC2	NW(120)/Geonet/ NW(140)	PP (geotextile), HDPE (geonet)	Thermally bonded	710 g/m ²	5

^aNW = nonwoven geotextile, W = woven geotextile, Na-bentonite = sodium bentonite, NW(200) = nonwoven geotextile (200 g/m²).

^bPP = polypropylene, PE = polyethylene, HDPE = high density polyethylene, PET = polyester.

^cThickness at 2 kPa for geotextiles and GCLs, at 20 kPa for geocomposites and geomembranes.

^dAsperity height (mm) measured through the scanning electron microscope (SEM). GMr2 presents two different textured sides: s1 = side 1 and s2 = side 2.

Table 2. Type of soils

Soil	Grain-size	w_L^a	I_p	MP ^b (γ_{max} ; w_{opt})	Direct shear parameters ($R^2 > 0.98$)			
					Friction angle (°)		Cohesion (kPa)	
					Peak	Residual	Peak	Residual
S1	90% fine 10% coarse	45	21	19.2 kN/m ³ ; 12%	37	34	48	0
S2	85% fine 15% coarse	37	17	20.6 kN/m ³ ; 8.5%	33	34	9	0
S3	90% fine 10% coarse	57	33.5	17.0 kN/m ³ ; 15%	25	26	17.5	0

^a w_L = liquid limit, I_p = plasticity index.

^bMP = modified proctor compaction was used, γ_{max} = maximum dry density.

w_{opt} = optimum water content corresponding to saturation degree of 85%.

1 mm/min for soil/GM. These different shear rates were used for the following reasons: on the one hand, the recommendation of the above-mentioned standard (see sections 10.7 and 11.6) was followed. On the other hand, for GT/GM interfaces, the studies of Stark *et al.* (1996), Triplett and Fox (2001) state that the shear rate does not significantly affect the peak and post-peak strength.

For soil/GM tests, the soil sample was compacted outside the machine applying a static vertical load with a hydraulic press to get the modified Proctor density.

First the normal stress was applied using a rigid loading platen, after 10 min of consolidation, the lower shear box was moved horizontally at a constant shear rate. The maximum horizontal displacement reached was 50 mm. The shear displacement, shear force and vertical displacement were recorded during the test. The shear force was measured using a suitable dynamometric ring. Two linear variable differential transformers (LVDTs) were used to measure horizontal and vertical displacements.

3. DIRECT SHEAR TESTS

3.1. Geotextile/geomembrane

3.1.1. Interface shear strength behaviour

All interfaces tested present frictional behaviour, which was modelled by Coulomb's equation $\tau = c_a + \sigma_n \cdot \tan(\delta)$, where τ and σ_n are interface shear strength and normal stresses acting on the failure plane, c_a is the interface adhesion and δ is the interface friction angle. Linear regression of the plot of τ against σ_n was used to identify the best-fit interface shear strength parameters. The shear strength of most interfaces tested in this investigation presented frictional parameters, that is, negligible or null adhesion and important friction angles.

A total of 90 direct shear tests of 18 different GT/GM interfaces (Table 3) were performed under wet conditions. The range of normal stress applied was 25–450 kPa. The peak interface shear strength was usually reached at 4–10 mm and the post-peak strength was obtained at 50 mm.

Table 3. Geotextile/geomembrane interfaces tested

Geotextile/geomembrane interfaces	Sample size (mm)	Normal stress (kPa)	Direct shear test conditions
GT1/GMs GT1/GMr1 GT1/GMr2s1 GT1/GMr2s2 GT1/GMr3 GT1/GMr4 GT2/GMs GT2/GMr1 GT2/GMr2s1 GT2/GMr2s2 GT2/GMr3 GT2/GMr4 GT3/GMs GT3/GMr1 GT3/GMr2s1 GT3/GMr2s2 GT3/GMr3 GT3/GMr4	300 × 285	25, 50, 100, 300, 450	Wet: <ul style="list-style-type: none"> • hydration time: geotextile 24 h, geomembrane 0 h • consolidation time: 10 min • shear rate: 5 mm/min

Table 5. Soil/geomembrane interfaces tested

Geotextile/geomembrane interfaces	Sample size (mm)	Normal stress (kPa)	Direct shear test conditions
S1/GMs S1/GMr1 S1/GMr2s1 S1/GMr3 S2/GMs S2/GMr1 S2/GMr2s1 S2/GMr3 S3/GMs S3/GMr1 S3/GMr3	200 × 200	100, 300, 500	Dry: <ul style="list-style-type: none"> • static compaction of soil off shear machine • consolidation time: 10 min. • shear rate: 1 mm/min

Table 4. Geocomposite/geomembrane interfaces tested

Geocomposite/geomembrane interfaces	Sample size (mm)	Normal stress (kPa)	Direct shear test conditions
GC1(200) ^a /GMs GC1(200)/GMr1 GC1(200)/GMr2s1 GC1(200)/GMr2s2 GC1(200)/GMr3 GC1(200)/GMr4 GC2(140) ^b /GMs GC2(140)/GMr1 GC2(140)/GMr2s1 GC2(140)/GMr2s2 GC2(140)/GMr3 GC2(140)/GMr4	300 × 285	25, 50, 100	Dry: <ul style="list-style-type: none"> • consolidation time: 10 min • shear rate: 5 mm/min

^aGC1(200)=GC1 was tested by the side of the NW of 200 gr/m².
^bGC2(140)=GC2 was tested by the side of the NW of 140 gr/m².

Figure 2a presents graphs of typical interface shear strength plotted against shear displacement for a non-woven geotextile/textured geomembrane interface (GT1/GMr2s1). Strain-softening behaviour can be observed (Byrne 1994; Stark *et al.* 1996; Jones and Dixon 1998) and the higher the normal stress, the higher the strain-softening behaviour (Bacas *et al.* 2011).

Approximately 60% of the tests revealed non-linear failure envelopes and 40% linear envelopes. Figure 2b shows non-linear peak and post-peak failure envelopes (continuous lines). However, the straight envelopes passing through the origin (dashed lines) with peak and post-peak friction angles of 23° and 10° also show a good fit ($R^2 > 0.9$).

In agreement with Giroud *et al.* (1990), Koutsourais *et al.* (1991), Stark *et al.* (1996), Hebler *et al.* (2005), McCartney *et al.* (2009) and Kim and Frost (2011), the interaction mechanism during the shear of geotextile/textured geomembrane presented two main components: one was the interlocking (hook and loop) between the individual filaments and the geomembrane roughness and the other was the friction between the materials. Figure 3 illustrates how these mechanisms developed at a superficial level (< 50 kPa) or at a geotextile matrix level, which depended on the normal stress.

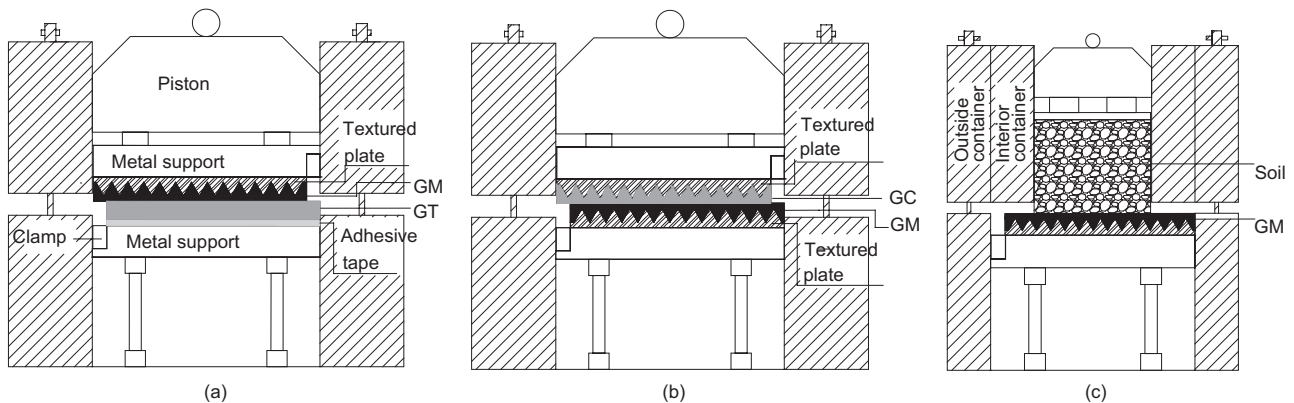


Figure 1. Sketch of large direct shear test: (a) GT/GM, (b) GC/GM and (c) Soil/GM

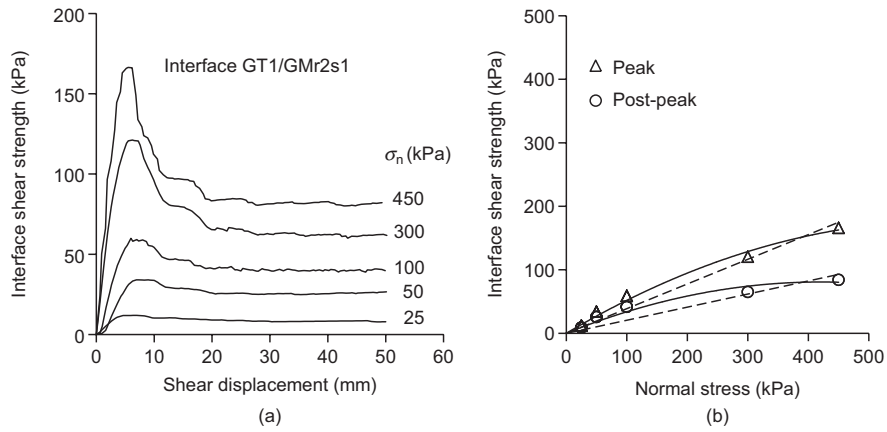


Figure 2. Interface needle-punched GT/textured GM: (a) interface shear strength plotted against shear displacement curves; (b) peak and post-peak failure envelopes

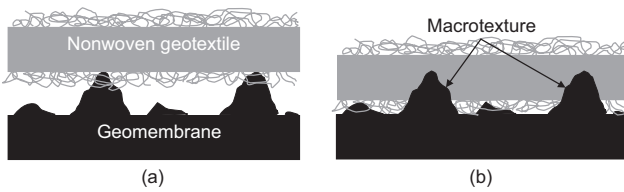


Figure 3. Interaction mechanisms between NW GT and textured GM at different normal stresses (cross shear direction section): (a) at low normal stress; (b) at high normal stress (after Hebler *et al.* 2005)

3.1.2. Influence of geomembrane roughness

Figure 4 presents graphs of the interface friction angles plotted against asperity height (mm), where the following aspects were observed: The smaller values belonged to the smooth geomembrane (GMs) and the interface shear strength was supplied by the friction mechanism; hence, the GT/GMs interfaces presented similar peak and post-peak friction angles.

The interlocking mechanism was directly affected by the roughness, increasing the peak interface shear strength as well as causing strain softening behaviour. Normally, the higher the asperity height and interlocking, the higher the peak interface shear strength (Ivy 2003; McCartney *et al.* 2005). Hence, GMr2s1 and GMr3 with asperity heights larger than 1 mm (Table 1) showed the greatest

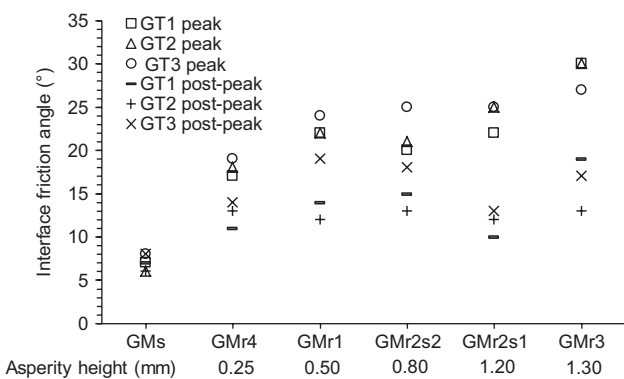


Figure 4. Interface friction angles of GT/GM interfaces

peak values. Similarly, GMr4 had the smallest asperity height and presented the smallest peak frictional angles. Furthermore, the interlocking increased with increasing normal stress (Bacas *et al.* 2011).

The post-peak values did not show a clear trend related to the size of the asperity, but show dependency on the type of geotextile (McCartney *et al.* 2005).

3.1.3. Influence of geotextile fibres

Figure 5 shows interface shear strength plotted against shear displacement curves at 50 kPa for the needle-punched geotextiles, GT1 and GT2. They were made of needle-punched monofilament and staple fibres, respectively (Table 1). It can be observed that the length of the fibres greatly affected the interface shear strength at low normal stress. GT2 presented the smaller interface shear strength values for both geomembranes, GMr1 and GMr3, whose macrotexture is smaller and greater than 1 mm, respectively. Thus, at a superficial level, the staple fibres of the GT2 did not develop an interlocking mechanism as strong as the monofilament of the GT1 did.

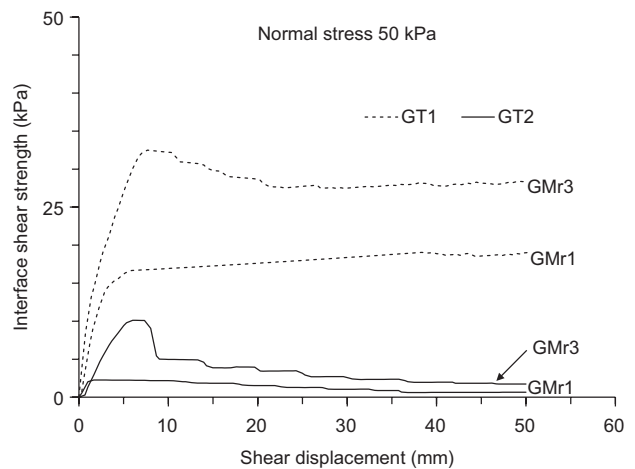


Figure 5. Interface shear strength plotted against shear displacement at low normal stress for needle-punched GT/textured GM interfaces

On the other hand, the influence of the manufacture of the geotextiles can be observed by comparing the nonwoven monofilament geotextiles GT1 and GT3 in Figure 4. The former is made by needle-punching and the latter is made by a heat bonding system. Figure 6 shows microscope pictures of these geotextiles. GT1 presents looser filaments and greater gaps than GT3, which shows higher interlocking, leading to higher interface shear strength.

Finally, the post-peak values seem to depend on the type of geotextile to some extent. Figure 4 shows that GT3 presented the largest post-peak values except for GMr3, because its heat-bonded monofilaments were stretched and very tangled during the shear, causing a higher resistance as the geomembrane brushed against the geotextile. GT2 on the other hand presented most of the lowest post-peak values because its staple fibres were stretched and brushed most easily.

One conclusion from these analyses is that the manufacturing process of the geotextile influences both the peak and the post-peak interface shear strength. If the geomembrane roughness is irregular and dense the use of heat-bonded monofilaments is recommended, because the interlocking mechanism has a big influence on interface shear strength. If, however, the roughness is regular and uniform then the use of needle-punched filaments is recommended, especially for high normal stress levels.

Finally, for cover systems of landfills subjected to low ranges of normal stresses, the use of monofilament rather than staple fibres are recommended, because the former mobilises the interlocking mechanism at lower normal stresses better than the latter.

3.2. Drainage geocomposite/geomembrane

3.2.1. Interface shear strength behaviour

The drainage GC/GM interfaces were tested with normal stress ranging from 25 to 100 kPa, which simulate the upper range of low normal stresses that typical cap and liner systems are subjected to. A total of 36 direct shear tests of 12 different drainage GC/GM interfaces (Table 4) were carried out under dry conditions. In addition, eight tests of geocomposites alone (GC1 and GC2) were performed in dry conditions. The peak interface shear strength was usually reached at 3–8 mm in line with Stark *et al.* (1996), the post-peak strength was reached at 50 mm.

Figure 7a presents curves of typical interface shear strength plotted against shear displacement for drainage of geocomposite/textured geomembrane interfaces, GC2 (140)/GMr3. The asperity height of GMr3 was > 1 mm. The drainage geocomposite GC2 had two needle-punched geotextiles, 120 and 140 g/m² (side tested), thermally bonded to a geonet (Table 1). These curves show that the reduction in shear stress at displacements beyond peak led to the typical strain softening behaviour

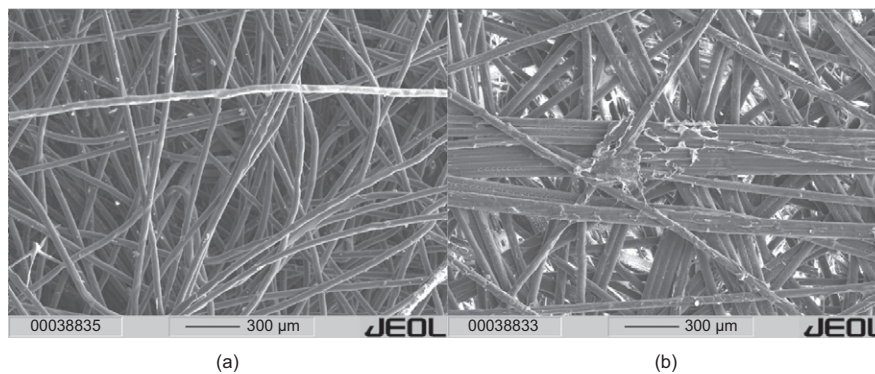


Figure 6. Scanning electron microscope (SEM) images of geotextiles: (a) GT1; (b) GT3

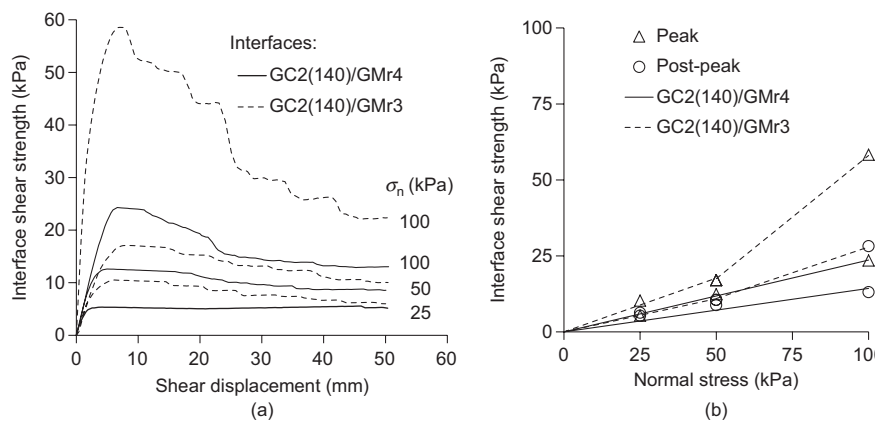


Figure 7. Interface drainage geocomposite/textured geomembrane: (a) interface shear strength plotted against shear displacement curves; (b) peak and post-peak failure envelopes

(Byrne 1994; Stark *et al.* 1996). The curve of 100 kPa presents a peak interface shear strength larger than the others. Although the data are limited, the failure envelope tends to be bilinear (Figure 7b), with the inflection point at normal stress of 50 kPa, indicating that beyond the normal stress of 50 kPa, the interaction mechanisms changed.

The analysis of the interface shear strength curves as well as the samples after testing resulted in the interaction mechanisms presented in Figure 8. As was the case for GT/GM interfaces, the interaction mechanisms depended on the normal stress applied. At low normal stress the interaction was mainly between the geotextile and the geomembrane, and therefore similar to the GT/GM interfaces described earlier. Figure 8a displays the interlocking (hook and loop) between geotextile filaments and geomembrane roughness and the friction mechanisms. Thus, the geonet does not significantly affect interface shear strength.

As normal stress increases, the geotextiles are compressed around the strands of the geonet, which is embedded into the geomembrane, as shown in Figure 8b. Therefore, the shear behaviour is frictional, similar to the geonet/geomembrane interfaces (Koutsourais *et al.* 1991; Byrne *et al.* 1992; Bergado *et al.* 2006), the interlocking mechanism hardly makes a difference. The friction takes place between the geonet strands and the geomembrane roughness (Giroud *et al.* 1990). The geonet aids the damage or removal of the roughness from the geomembrane as Stark *et al.* (1996) also pointed out.

The failure plane occurred between the geotextile of the drainage geocomposite and the geomembrane. However,

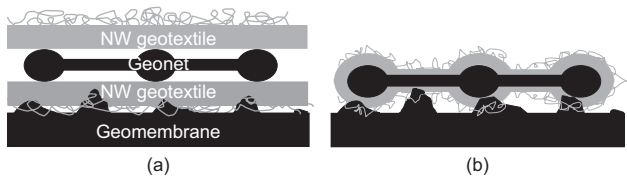


Figure 8. Interaction mechanisms between drainage geocomposite and textured GM (cross shear direction section): (a) at low normal stress; (b) at high normal stress

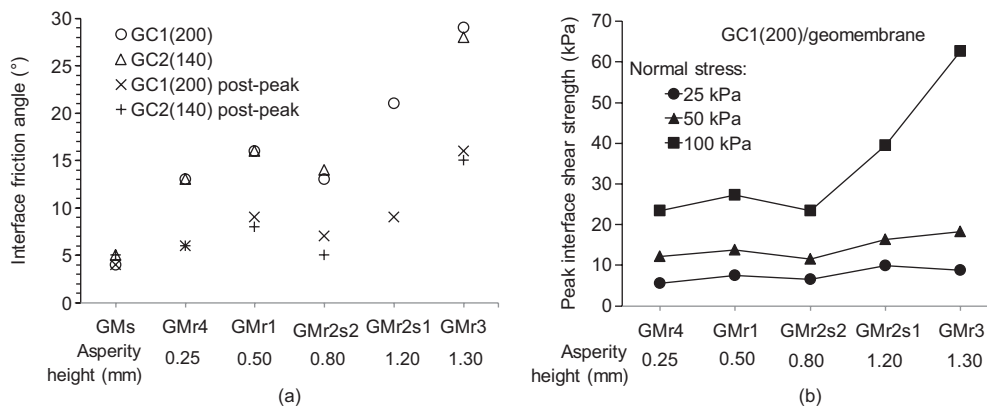


Figure 9. (a) Interface friction angle of drainage geocomposite/geomembrane; (b) peak interface shear strength plotted against asperity height

for GC/GMr3 interfaces at normal stress of 100 kPa the failure plane was inside the drainage geocomposite, between the geonet and the geotextile. Due to this fact, GC1 and GC2 were tested alone. The peak secant friction angles at 100 kPa were 28° and 26°, respectively. These values are smaller than the peak secant friction angles of GC1(200)/GMr3 and GC2(140)/GMr3, 32° and 30°, confirming the internal geocomposite weakness plane.

3.2.2. Influence of geomembrane roughness

Figure 7 presents the results of two types of interfaces: GC2(140)/GMr4 and GC2(140)/GMr3. The asperity height of GMr4 was < 1 mm and GMr3 was > 1 mm. GMr3 exhibited higher interface shear strength than GMr4. The failure envelopes of GMr3 were bilinear but GMr4 had a linear failure envelope for the normal stress range tested. This was due to the fact that geomembranes with asperities smaller than 1 mm presented the inflexion point at a higher normal stress (> 100 kPa) than geomembranes with asperities larger than 1 mm (50 kPa), as can be observed in Figure 9b. GMr1, GMr2s2 and GMr4 present similar interface shear strengths and linear envelopes, increasing the interface shear strength proportionally to the normal stress. However, GMr2 and GMr3 do not; they exhibit bilinear failure envelopes.

Figure 9a presents the friction angles of the drainage GC/GM interfaces tested plotted against asperity height. These friction angles were within the range of the values presented by Stark *et al.* (1996). The results prove that the geomembrane roughness increased the interface shear strength: the higher the asperity height, the higher the shear strength. This fact is more noticeable when the roughness was larger than 1 mm.

3.3. Soil/geomembrane

3.3.1. Interface shear strength behaviour

The soil/GM interfaces were tested at normal stress of 100, 300 and 500 kPa, simulating the range of normal stresses that typical liner systems are subject to. A total of 33 direct shear tests of 11 soil/GM interfaces were performed in dry conditions (Table 5). The soil samples were 200 mm long, 200 mm wide and 50 mm high. They were compacted outside the direct shear machine to get the

modified Proctor density and the optimum water content (Table 2). However, in real conditions, the soil was directly compacted on the geosynthetic, which can affect to the results at low normal stress.

The peak interface shear strength was usually reached at 3–8 mm (Stark and Poeppel 1994), the post-peak strength was measured at 50 mm.

Figure 10a presents the typical interface shear strength – shear displacement curves for the interfaces S1/GMr3 and S1/GMr1. The interface shear strength curves present strain-softening behaviour, as described in previous interfaces (GT/GM and drainage GC/GM). The interface shear strength reaches its peak when the asperities move the soil over them. Then, the strength goes down because the remoulded soil resists less. Figure 10b shows the straight failure envelopes for high normal stresses. The peak and post-peak friction angles were 29° and 20° for S1/GMr3, 31° and 27° for S1/GMr1.

All test results analysed and the observation of the samples after testing show the interaction mechanisms developed during shearing. These interaction mechanisms followed the same rules as GT/GM and drainage GC/GM interfaces. Figure 11 illustrates different behaviours at low and high normal stress. At the low normal stress tested, 100 kPa, the asperities slightly embedded into the soil. Thus, the interface shear strength was mainly supplied by the sliding between asperities and the soil at a superficial level. However, it is noteworthy that this behaviour may be affected by the way the soil was compacted. As the normal stress increased (> 100 kPa), the soil was entirely embedded between the asperities, and interface shear

strength came from a friction mechanism developed in two ways: one was the internal shear strength of the soil itself placed above the geomembrane and the other was the friction between the asperities and the soil, as indicated in Figure 11b, that is, the sliding and ploughing effect reported by Zettler *et al.* (2000).

3.3.2. Influence of geomembrane roughness

Figure 10 shows the results of the interfaces S1/GMr1 and S1/GMr3. GMr1 has an irregular heavily textured surface smaller than 1 mm. GMr3 has regular asperities larger than 1 mm. GMr1 reached greater interface shear strength than GMr3. The roughness of GMr1 was almost entirely embedded into the soil, which caused the interface shear strength to be mainly supplied by the internal shear strength of the soil itself. The shear plane was inside the soil as shown in Figure 12a (Koerner *et al.* 1986; Mitchell and Mitchell 1992; Orman 1994). However, the roughness of GMr3 led to a ploughing effect, mobilising the internal shear strength of the soil and the friction of the soil-roughness contacts, which remoulded the soil and resulted in smaller post-peak values (Zettler *et al.* 2000). In this case, the shear plane was between the soil and the geomembrane as shown in Figure 12b.

Figure 13 presents the friction angles of the soil/GM interfaces tested, observing that evidently, the smooth geomembrane offered the smallest interface shear strength. The peak friction values were between 6° and 11° and the post-peak ones between 3° and 8°. These values are in line with the data shown by Seed and Boulanger (1991), Koerner *et al.* (1986), Stark and

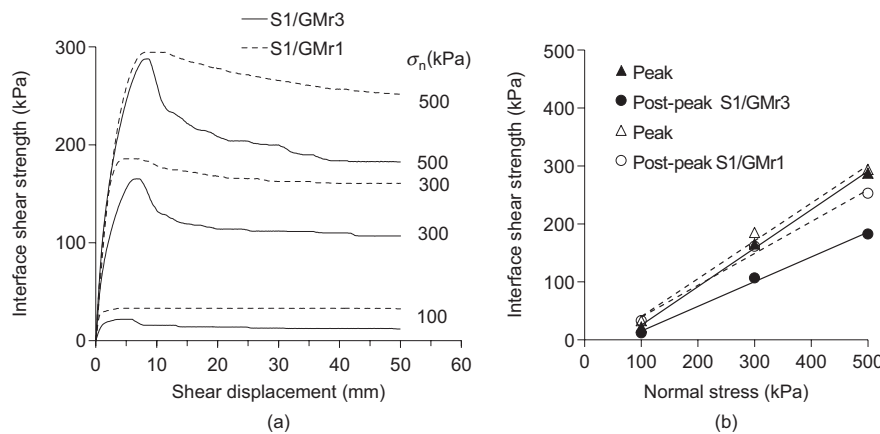


Figure 10. Interfaces S1/GMr3 and S1/GMr1: (a) interface shear strength shear plotted against displacement curves; (b) peak and post-peak failure envelopes

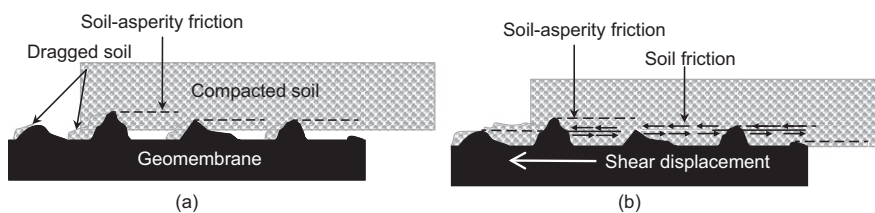


Figure 11. Interaction mechanisms between the soil and the textured geomembrane (shear direction section): (a) at low normal stress; (b) at high normal stress

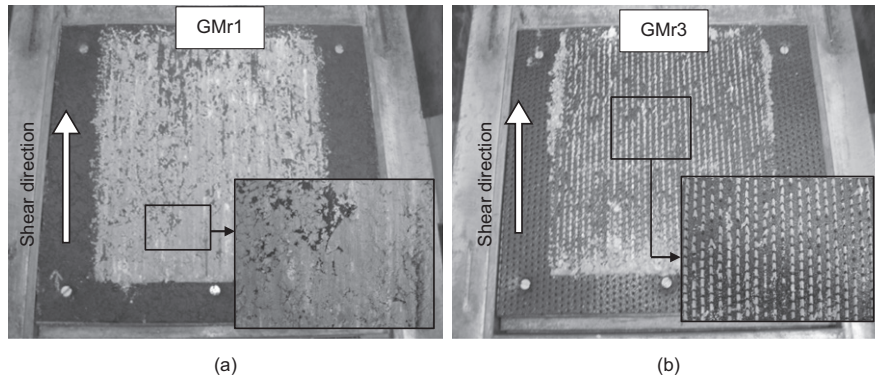


Figure 12. GMr1 and GMr3 samples after testing with S1 at normal stress of 500 kPa

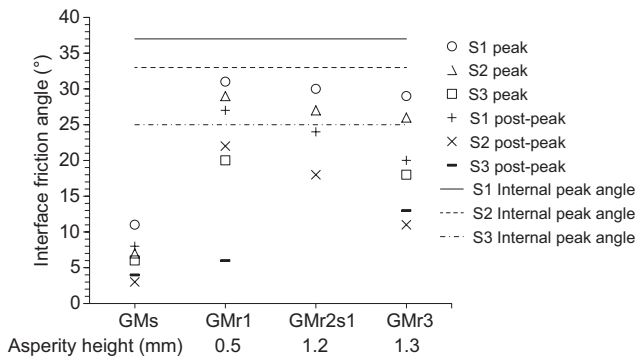


Figure 13. Interface friction angles of soil/GM interfaces and compacted soils

Poeppl (1994) and Bergado *et al.* (2006). In this case, the post-peak strength was caused by the polishing of the smooth geomembrane during the shear and the damage on its surface. This damage was caused by the friction of coarser particles within the clayed soil (Zettler *et al.* 2000; Sharma *et al.* 2007). These facts were observed in the visual inspection of the samples after testing.

The peak friction angles of the compacted soil/textured geomembrane interfaces were between 18° and 32°, in line with data from Mitchell and Mitchell (1992). The post-peak angles were between 6° and 27°. GMr1 usually yielded the largest peak values, because most of the friction was provided by the soil itself. GMr2s1 presented slightly larger values than GMr3, because the asperity of GMr2s1 was less dense (4 units/cm²) than that of GMr3 (9 units/cm²). This means that there was more soil between the asperities of GMr2s1 than between that of GMr3, and hence the former moved more soil friction, causing larger peak values.

3.3.3. Influence of type of soil

Small direct shear tests were carried out with the different soils, S1, S2 and S3 to analyse their effects on the interfaces. The sample dimensions were 60 mm long × 60 mm wide × 29 mm height. The normal stresses applied were 100, 200 and 300 kPa and the constant shear rate was 0.006 mm/min. The soil samples were prepared by modified Proctor density and water content (Table 2).

Figure 13 shows that the soil S1 presented the largest peak interface friction angles, 37°. Furthermore, these results show that the largest interface friction angles belonged to S1/geomembranes, whose peak values were between 29° and 32° and post-peak values were between 20° and 27°. Note that these values did not exceed the angles of internal shear strength of the soil S1 itself (Koerner *et al.* 1986; Koutsourais *et al.* 1991; Mitchell and Mitchell 1992; Stark and Poeppl 1994; Bergado *et al.* 2006).

The soil S3 (*I_p* = 34), which was more clayed than the soils S1 (*I_p* = 21) and S2 (*I_p* = 17), presented the lowest peak angle of friction, 25°, as well as the lowest peak friction angles of S3/geomembrane interfaces, 18° to 20°, and the lowest post-peak values, 6° to 13°. These findings prove that the internal shear strength of soil was the main interaction mechanism supplying interface shear strength at high normal stress, as also pointed out by Koerner *et al.* (1986) and Mitchell and Mitchell (1992).

3.4. Comparison of peak friction angles

Figure 14 compares the peak interface friction angles, which were from lowest to highest: drainage in the order GC/GM, GT/GM and soil/GM.

An exception to this were the interfaces formed with the geomembrane GMr3, which showed similar values with the geotextiles and the drainage geocomposites tested and the compacted soils S1 and S2. The only exception was the

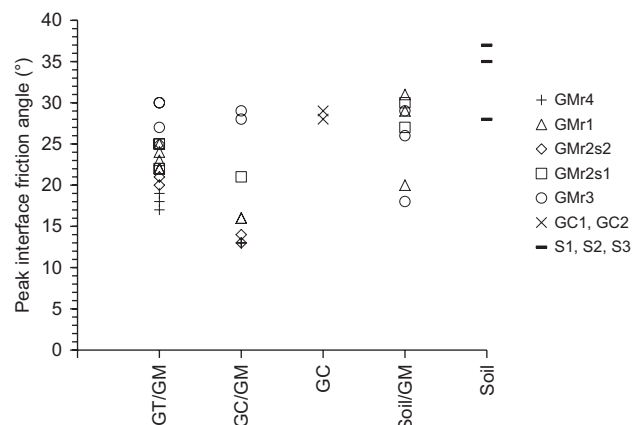


Figure 14. Comparison of peak friction angles between interfaces

compacted soil S3 that presented the lowest values due to its larger plasticity index.

4. CONCLUSIONS

Large direct shear tests were conducted on three critical interfaces typically used for lined containment facilities: GT/GM, drainage GC/GM and soil/GM. The following main conclusions are derived from this study.

- (a) The interface shear interaction mechanisms depend on the normal stress, for GT/GM interfaces, the interlocking and friction mechanisms take place at a superficial level at low normal stress (< 50 kPa) and at a matrix level at high normal stress (> 50 kPa). For drainage GC/GM interfaces, the interlocking and friction mechanism appeared at low normal stress (< 50 kPa). However, only the friction mechanism appears at high normal stress (> 50 kPa). For soil/GM interfaces, the friction mechanism appeared at low normal stress (< 100 kPa) and internal soil friction at high normal stress (> 100 kPa).
- (b) For GT/GM interfaces, the peak interface shear strength mainly depended on the roughness of the geomembrane. Whereas post-peak interface shear strength appeared to depend on the type of geotextile. Usually the geotextiles made with staple fibres presented smaller post-peak values than monofilaments.
- (c) If the roughness of the geomembrane is irregular and dense it is recommended that nonwoven geotextile made of monofilaments was used, because it develops a larger interlocking mechanism causing the interface shear strength to increase.
- (d) If the roughness of the geomembrane is regular and evenly spread it is recommended to use the nonwoven geotextile with needle-punched filaments, especially for high normal stresses.
- (e) For cover systems of landfills subject to low normal stresses, it is recommend that monofilaments be used rather than staple fibres, since the former mobilises the interlocking mechanism at lower normal stresses.
- (f) For drainage GC/GM interfaces, the shape of the interface shear strength failure envelope depends on the asperity height of the textured geomembrane. If the asperity is smaller than 1 mm the failure envelope is linear, but if the asperity is larger than 1 mm it is bilinear.
- (g) The comparison of peak friction angles of the geosynthetic interfaces tested usually showed the following interfaces from most critical to least critical: drainage GC/GM, GT/GM and soil/GM.

ACKNOWLEDGEMENTS

This work was derived from an extensive research project sponsored by the Company Ferrovial S.A. (Spain) and conducted by the Geotechnical Group at the Civil Engineering School at University of Cantabria (Spain).

The facilities provided for this research project are gratefully acknowledged. Moreover, the authors are grateful to Deutscher Akademischer Austausch Dienst (DAAD, Germany) for the research fellowship received, as well as the facilities provided by the Chair for Rock Mechanics at the Geotechnical Institute at the Technical University Bergakademie Freiberg, Germany.

NOTATION

Basic SI units are given in parentheses.

c_a	adhesion of interface (Pa)
I_p	plasticity index (dimensionless)
δ	interface friction angle (degrees)
σ_n	normal stress (Pa)
τ	interface shear strength (Pa)

ABBREVIATIONS

GT	geotextile
GM	geomembrane
GC	drainage geocomposite
GT1, GT2, GT3	geotextile type 1, 2, 3
GMr1, GMr3, GMr4	geomembrane type 1, 3, 4
GMr2s1, GMr2s2	geomembrane type 2 side 1, side 2
GC1, GC2	drainage geocomposite type 1, 2
S1, S2, S3	soil type 1, 2, 3

REFERENCES

- ASTM D5321 *Standard Test Method for Determining the Coefficient of Soil and Geosynthetic or Geosynthetic and Geosynthetic Friction by Direct Shear Method*. ASTM International, West Conshohocken, PA, USA.
- Bacas, B. M., Konietzky, H., Cañizal, J. & Sagasetta, C. (2011). A new constitutive model for textured geomembrane/geotextile interfaces. *Geotextiles and Geomembranes*, **29**, No. 2, 137–148.
- Bergado, D. T., Ramana, G. V., Sia, H. I. & Varun, R. (2006). Evaluation of interface shear strength of composite liner system and stability analysis for a landfill lining system in Thailand. *Geotextiles and Geomembranes*, **24**, No. 6, 371–393.
- Brachman, R. W. I. & Sabir, A. (2013). Long-term assessment of a layered-geotextile protection layer for geomembranes. *Journal of Geotechnical and Geoenvironmental Engineering*, **139**, No. 5, 752–764.
- Briançon, L., Girard, H. & Gourc, J. P. (2011). A new procedure for measuring geosynthetic friction with an inclined plane. *Geotextiles and Geomembranes*, **29**, No. 5, 472–482.
- Byrne, R. J. (1994). Design issues with strain-softening interfaces in landfill liners. *Proceedings of Waste Technology '94*, Charleston, SC, USA, Session 4, Paper 4.
- Byrne, R. J., Kendall, J. & Brown, S. (1992). Cause and mechanism of failure, Kettleman Hills Landfill B-19, Phase IA. In *Stability of Slopes and Embankments II*, Seed, R. B. & Boulanger, R. W., Editors, American Society of Civil Engineers, New York, NY, USA, Geotechnical Special Publication no. 31, vol. 2, pp. 1188–1215.
- Eid, H. T. (2011). Shear strength of geosynthetic composite systems for design of landfill liner and cover slopes. *Geotextiles and Geomembranes*, **29**, No. 3, 335–344.

- Eid, H. T., Stark, T. D. & Doerfler, C. K. (1999). Effect of shear displacement rate on internal shear strength of a reinforced geosynthetic clay liner. *Geosynthetics International*, **6**, No. 3, 219–239.
- Fox, P. J. & Kim, R. H. (2008). Effect of progressive failure on measured shear strength of geomembrane/GCL interface. *Journal of Geotechnical and Geoenvironmental Engineering*, **134**, No. 4, 459–469.
- Fox, P. J. & Ross, J. D. (2011). Relationship between NP GCL internal and HDPE GMX/NP GCL interface shear strengths. *Journal of Geotechnical and Geoenvironmental Engineering*, **137**, No. 8, 743–753.
- Fox, P. J. & Stark, T. D. (2015). State-of-the-art report: GCL shear strength and its measurement – ten-year update. *Geosynthetics International*, **22**, No. 1, 3–47.
- Fox, P. J., Rowland, M. G., Scheithe, J. R., Davis, K. L., Supple, M. R. & Crow, C. C. (1997). Design and evaluation of a large direct shear machine for geosynthetic clay liners. *Geotechnical Testing Journal*, **20**, No. 3, 279–288.
- Fox, P. J., Rowland, M. G. & Scheithe, J. R. (1998). Internal shear strength of three geosynthetic clay liners. *Journal of Geotechnical and Geoenvironmental Engineering*, **124**, No. 10, 933–944.
- Fox, P. J., Ross, J. D., Sura, J. M. & Thiel, R. S. (2011). Geomembrane damage due to static and cyclic shearing over compacted gravelly sand. *Geosynthetics International*, **18**, No. 5, 272–279.
- Gilbert, R. B. & Byrne, R. J. (1996). Strain-softening behavior of waste containment system interfaces. *Geosynthetics International*, **3**, No. 2, 181–202.
- Giroud, J. P. & Darrasse, J. (1993). Hyperbolic expression for soil-geosynthetics or geosynthetics-geosynthetic interface shear strength. *Geotextiles and Geomembranes*, **12**, No. 3, 275–286.
- Giroud, J. P., Swan, R. H., Richer, P. J. & Spooner, P. R. (1990). Geosynthetic landfill cap: Laboratory and field tests, design and construction. In *Proceedings of the 4th International Conference on Geotextiles, Geomembranes and Related Products*, Den Hoedt, G., Editor, Balkema, Rotterdam, the Netherlands, pp. 493–498.
- Hebeler, G. L., Frost, J. D. & Myers, A. T. (2005). Quantifying hook and loop interaction in textured geomembrane-geotextile systems. *Geotextiles and Geomembranes*, **23**, No. 1, 77–105.
- Ivy, N. (2003). Asperity height variability and effects. *GFR*, **21**, October–November, 28–29.
- Jones, D. R. V. & Dixon, N. (1998). Shear strength properties of geomembrane/geotextile interfaces. *Geotextiles and Geomembranes*, **16**, No. 1, 45–71.
- Kim, D. & Frost, J. D. (2011). Effect of geotextile constraint on geotextile/geomembrane interface shear behavior. *Geosynthetics International*, **18**, No. 3, 104–123.
- Koerner, R. M., Martin, J. P. & Koerner, G. R. (1986). Shear strength parameters between geomembranes and cohesive soils. *Geotextiles and Geomembranes*, **4**, No. 1, 21–30.
- Koutsourais, M. M., Sprague, C. J. & Pucetas, R. C. (1991). Interfacial friction study of cap and liner components for landfill design. *Geotextiles and Geomembranes*, **10**, No. 5–6, 531–548.
- Liu, H. & Martinez, J. (2014). Creep behavior of sand-geomembrane interfaces. *Geosynthetics International*, **21**, No. 1, 83–88.
- McCartney, J. S., Zornberg, J. G. & Swan, R. H. (2005). Effect of geomembrane texturing on GCL–geomembrane interface shear strength. In *Waste Containment and Remediation – GeoFrontiers 2005*, Alshawabkeh, A., Benson, C. H., Culligan, P. J., Evans, J. C., Gross, B. A., Narejo, D., Reddy, K. R., Shackelford, C. D. & Zornberg, J. G., Editors, American Society of Civil Engineers, Reston, VA, USA, Geotechnical Special Publication no. 142 (CD-ROM).
- McCartney, J. S., Zornberg, J. G. & Swan, R. H. (2009). Analysis of a large database of GCL–geomembrane interface shear strength results. *Journal of Geotechnical and Geoenvironmental Engineering*, **135**, No. 2, 209–223.
- Mitchell, R. A. & Mitchell, J. K. (1992). Stability evaluation of waste landfills. In *Stability of Slopes and Embankments II*, Seed, R. B. & Boulanger, R. W., Editors, American Society of Civil Engineers, New York, NY, USA, Geotechnical Special Publication no. 31, vol. 2, pp. 1152–1187.
- Orman, M. E. (1994). Interface shear strength properties of roughened HDPE. *Journal of Geotechnical Engineering*, **120**, No. 4, 758–761.
- Palmeira, E. M. (2009). Soil–geosynthetic interaction: Modelling and analysis. *Geotextiles and Geomembranes*, **27**, No. 5, 368–390.
- Pitanga, H. N., Gourc, J. P. & Vilar, O. M. (2009). Interface shear strength of geosynthetics: Evaluation and analysis of inclined plane tests. *Geotextiles and Geomembranes*, **27**, No. 6, 435–446.
- Sayeed, M. M. A., Janaki Ramaiah, B. & Rawal, A. (2014). Interface shear characteristics of jute/polypropylene hybrid nonwoven geotextiles and sand using large size direct shear test. *Geotextiles and Geomembranes*, **42**, No. 1, 63–68.
- Seed, R. B. & Boulanger, R. W. (1991). Smooth HDPE-clay liner interface shear strengths: compaction effects. *Journal of Geotechnical Engineering*, **117**, No. 4, 686–693.
- Sharma, J. S., Fleming, I. R. & Jogi, M. B. (2007). Measurement of unsaturated soil-geomembrane interface shear-strength parameters. *Canadian Geotechnical Journal*, **44**, No. 1, 78–88.
- Stark, T. D. & Poeppel, A. R. (1994). Landfill liner interface strengths from torsional-ring-shear tests. *Journal of Geotechnical Engineering*, **120**, No. 3, 597–615.
- Stark, T. D., Williamson, T. A. & Eid, H. T. (1996). HDPE geomembrane/geotextile interface shear strength. *Journal of Geotechnical Engineering*, **122**, No. 3, 197–203.
- Tripllett, E. J. & Fox, P. J. (2001). Shear strength of HDPE geomembrane/geosynthetic clay liner interfaces. *Journal of Geotechnical and Geoenvironmental Engineering*, **127**, No. 6, 543–552.
- Vieira, C. S., Lopes, M. L. & Caldeira, L. M. (2013). Sand-geotextile interface characterization through monotonic and cyclic direct shear tests. *Geosynthetics International*, **20**, No. 1, 26–38.
- Wasti, Y. & Özdüzgün, Z. B. (2001). Geomembrane-geotextile interface shear properties as determined by inclined board and direct shear box tests. *Geotextiles and Geomembranes*, **19**, No. 1, 45–57.
- Zettler, T. E., Frost, J. D. & Dejong, J. T. (2000). Shear-induced changes in smooth HDPE geomembrane surface topography. *Geosynthetics International*, **7**, No. 3, 243–267.
- Zornberg, J. G., McCartney, J. S. & Swan, R. H. (2005). Analysis of a large database of GCL internal shear strength results. *Journal of Geotechnical and Geoenvironmental Engineering*, **131**, No. 3, 367–380.

The Editor welcomes discussion on all papers published in *Geosynthetics International*. Please email your contribution to discussion@geosynthetics-international.com by 15 April 2016.